Blockchain based Privacy-Preserved Federated Learning for Medical Images: A Case Study of COVID-19 CT Scans

Rajesh Kumar[a], WenYong Wang[b,*], Cheng Yuan[d], Jay Kumar[a], Zakria[c], Chengyu Zheng[e], Abdullah Aman Khan[c]

[a]Yangtze Delta Region Institute (Huzhou), University of Electronic Science and Technology of China, Huzhou 313001, China.
[b]International Institute of Next Generation Internet, Macau University of Science and Technology, Taipa, 999078, Macau
[c]School of Software Engineering, University of Electronic Science and Technology of China, Chengdu, 611731, China.
[d]Materials Science and Engineering, Southwest Jiaotong University, Chengdu, 611731, China.
[e]China Telecommunications Corporation, Sichuan Branch , Chengdu 611731, China

ARTICLE INFO

ABSTRACT

Medical health care centers are envisioned as a promising paradigm to handle the massive volume of data of COVID-19 patients using artificial intelligence (AI). Traditionally, AI techniques often require centralized data collection and training the model in a single organization, which is most common weakness due to the privacy and security of raw data communication. To solve this challenging task, we propose a blockchain-based federated learning framework that provides collaborative data training solutions by coordinating multiple hospitals to train and share encrypted federated models without leakage of data privacy. The blockchain ledger technology provides the decentralization of federated learning model without any central server. The proposed homomorphic encryption scheme encrypts and decrypts the gradients of model to preserve the privacy. More precisely, the proposed framework: i) train the local model by a novel capsule network to segmentation and classify COVID-19 images, ii) then use the homomorphic encryption scheme to secure the local model that encrypts and decrypts the gradients, and finally the model is shared over a decentralized platform through proposed blockchain-based federated learning algorithm. The integration of blockchain and federated learning leads to a new paradigm for medical image data sharing in the decentralized network. The conducted experimental results demonstrate the performance of the proposed scheme.

1. INTRODUCTION

The drastic spread of novel coronavirus (COVID-19) around the globe has caused a large number of deaths in a year. The COVID-19 virus causes acute respiratory disease, which directly infects the human lungs, resulting in intensive breathing difficulty. Due to the highly contagious nature, COVID-19 detection remains among high-priority tasks. Currently, various artificial intelligence (AI) techniques are under exploration to discover better solutions to detect it Kumar et al. (2021a,b); Deng et al. (2021); Khan et al. (2020). Particularly, a significant portion of the research is focused on CT scan images in the past year as it proved to be a more reliable source to detect the infection. However, these techniques often require a large

*Corresponding author: Wenyong Wang Tel.: +86-139-0801-4292;
e-mail: rajakumarlohano@gmail.com (Rajesh Kumar), wywang@must.edu.mo (WenYong Wang), chy@my.swjtu.edu.cn (Cheng Yuan), jay_tharwani1992@yahoo.com (Jay Kumar), zakria.uestc@hotmail.com (Zakria), 18081000808@189.cn (Chengyu Zheng), abdkhan@hotmail.com (Abdullah Aman Khan)

amount of data from a single source (hospital or research center) to train the classification model to predict more accurately. In contrast, data from a single source lacks the feature distribution variance. TThe less variation in data directly leads to sampling error and high model loss, affecting the diagnosis results in terms of accuracy. The data variation problem can be solved if many hospitals can share the data. However, the reason data confidentiality and privacy restrict multiple hospitals to share the data to train the model. Due to this issue, traditional learning, where only local data is considered, may not fit properly. In contrast, the transfer learning enables sharing the model instead of sharing the data. The transfer learning exploit a general pre-trained model and modifies it with accordance to local data Das et al. (2020); Pathak et al. (2020); Deng et al. (2020). Yet, the sensitivity of a local model totally depends on the quality of the pre-trained model. Let us take a scenario in a rural area hospital with insufficient data to train the model. However, the hospital can collaborate with another hospital while considering the same goal without sharing the data. However, transfer learning still confines the base model to increase more robustness while taking benefit from local data of the hospital. Due to this reason, hospitals are unable to get the full benefit from AI.

Recently, the federated learning technique is introduced to solve the problem by collaboratively training the model without physically exchanging the model itself. The collaborative model solves the data variance issue and enables the evolution of the model over time for all hospitals. Generally, it is a collaborative learning framework of federated learning which enables multiple collaborators to train their local model and send the learned weights to a centralized server where they are aggregated into a global model. This procedure of gaining knowledge is in the form of a consensus model without moving patient data beyond the firewalls of parent data recording centers (hospital or research center). To this point, the learning process occurs locally at each participating institution, and only the model characteristics are transferred to a federated server for global model training. Originally federated learning was developed for different domains, such as distributed learning, edge device, and mobile computing Yang et al. (2019); Thomas et al. (2018). Due to its vast scope of applicability, it has gained considerable research attention for healthcare applications Blanquer et al. (2020); Yang et al. (2021); Thwal et al. (2021); Malekzadeh et al. (2021a,b); Li et al. (2020); Baheti et al. (2020); Lee and Shin (2020); Huang et al. (2019); Brisimi et al. (2018); Can and Ersoy (2021). Recent research has proven that models trained by federated learning can achieve a comparable levels of performance to ones trained on centrally hosted medical data Can and Ersoy (2021); Dinh et al. (2021); Cheng et al. (2020); Yang et al. (2020). However, still there exist security issue of federated learning Shokri and Shmatikov (2015), where the users can share the gradients to verify the security and privacy of the data. To this end, their methodology was exposed to vulnerability even for passive attackers Dai et al. (2019); Tang et al. (2018).

To tackle the security and scalability issues, the blockchain as a ledger technology is attractive to provide model decentralization without involving any central server. Particularly

blockchain provides the facility to collect the data model securely from the different points or locations (i.e., Japan, China, Pakistan, USA, UK) to train the global model. The recent works focus on federated learning using central server topology Blanquer et al. (2020); Yang et al. (2021); Thwal et al. (2021); Malekzadeh et al. (2021a,b); Li et al. (2020); Baheti et al. (2020); Lee and Shin (2020); Huang et al. (2019); Brisimi et al. (2018); Can and Ersoy (2021). However, none of the above considers blockchain-based federated learning to decentralize the global model in medical image analysis. Therefore, there still exist the gap between secure federated learning without the dependency of a central server to provide secure model sharing and trust issue for data providers (e.g., hospital).

Motivated by a current situation where the model needs to update continuously to deal with new types of COVID-virus over time while considering the above-discussed issues. In this paper, we propose a framework that integrates privacy-preserving federated learning over the decentralized blockchain. To train the local model, we design a capsule network based on segmentation and classification to detect the COVID-19 images. Our segmentation network aims to extract nodules from the chest CT images. For each locally trained model, gradients are encrypted using a homomorphic encryption technique to preserve the privacy of each hospital. In this encryption technique, the hospitals are assigned the same secret key to reducing the communication overhead for high-dimensional data in neural networks. In this way, the client's or users' side encryption knowledge, which guarantees user privacy and blockchain, ensures the data's reliability. The task of aggregation and learning the global model is trained over the blockchain. We exploit the Direct Acyclic Graph (DAG) to reduce the computation efficiency of the blockchain. The main contributions of this paper are summarized as follows:

1. We design blockchain based federated-learning framework which provides collaborative data training and decentralization of federated learning model without any central server.

2. We designed a homomorphic encryption scheme for encrypting the weights of the local model, which can ensure the hospital data's privacy.

3. We design a blockchain based federated learning algorithm to build data models and sharing the data models instead of raw data. It aggregate the local model weights and train the global model.

4. For local model training, we propose an Capsule Network model for segment pneumonia infection regions and automatically classify the COVID-19 chest CT images.

5. The proposed framework update model continuously to deal with new types of COVID-virus and easily share the latest information of the patients through out the world.

The rest of the paper is arranged as follows. Section 2 discuss and introduce the basic knowledge of the deep learning and blockchain technology. In Section 3 , discuss the system model, COVID-19 CT image detection framework, then design a protocol for encryption gradients. Finally, blockchain based federated learning model. Then , we discuss the performance
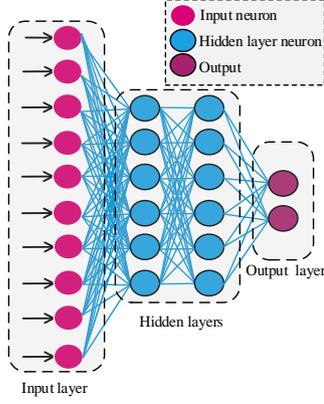
Fig. 1: Background of Basic Deep Learning Model

analysis and security analysis in Section 4. Finally, we concludes this work in Section 5.

2. PRELIMINARIES

This section briefly introduces the fundamentals of deep learning, federated learning, homomorphic encryption, and blockchain-based federated learning model, which is followed by the system model. The main mathematical notations used in this article are listed in Table 1.

Table 1: Summary of the notations

Notations	Description
$W_i(a)$	Local model weights
$m_i(t)$	local model learned by devices
CW	The cumulative weight of tr
W	weights of the model
$P_{x,y}$	The transition probability of transactions
λ	The 0 an 1 selection state
$\mathbb{Z}_{\mathbb{N}}$	Plaintext space
$\mathbf{A} \xrightarrow{\$} \mathbb{Z}_p^{\kappa \times \tau}$	Matrix
g	Gradients vector for the model
pk/sk	Public/Private key
$\otimes$	Product between two ciphertexts

2.1. Deep Learning

The deep learning models are used the feedforward and backpropagation algorithms to train the model shown in Figure 1. The feedforward function defined as $f(x, w) = y^-$, where x shows the input vector and w represents the parameter vector. The $D = (x_i, y_i); i \in I$ is the training dataset for the each instance of (x_i, y_i) . Moreover l is the loss function , whereas the training dataset D on loss function defined as $L(D, w) = \frac{1}{|D|} \sum_{(x_i, y_i) \in D} l(y_i, f(x_i, w))$. However, the backpropagation phase utilized the stochastic gradient descent (SGD) for updating the parameters.

$$\mathbf{w}^{t+1} \leftarrow \mathbf{w}^t - \eta \nabla_{\mathbf{w}} L\left(D^t, \mathbf{w}^t\right) \quad (1)$$

where η learning rate of the hyperparameter and w^t defined as vector of i_{th} iteration. However, D^t is the training dataset. Equation 1 shows the standard training procedure to train the data for the one hospitals or users.

2.2. Federated Learning

Federated learning is a distributed and secure deep learning technique that enables training a shared model without leakage the hospitals privacy. Moreover, federated learning has introduced a mechanism to collect the data from various parties or hospitals without leakage the hospitals privacy. The advantage of the federated learning model is reducing the resources (i.e., memory, power) consummation of a single participant and improving the quality of the training model. In other words, federated learning learn the model collaboratively and share the trained model in the local machines. More detail, each users $u \in U$ has own private dataset $D_u \subseteq D$. The equation for the mini-batch dataset $D^t = \bigcup_{u \in U} D_u^t$ with SGD shown below

$$\mathbf{w}^{t+1} \leftarrow \mathbf{w}^t - \eta \frac{\sum_{u \in u} \nabla_{\mathbf{w}} L\left(D_u^t, \mathbf{w}^t\right)}{|U|} \quad (2)$$

Each user shares the local model to the blockchain distributed ledger for training the global shared model. Then, the users / hospitals upload the new data, i.e., (gradients or weights) for updating the global model. Moreover, each user $u \in U$ has own private dataset with data samples for federated learning which is shown in Figure 2.

$$F_i(w) = \frac{1}{|D_i|} \sum_{j \in D_i} f_j(w, x_i, y_i) \quad (3)$$

For multiple devices or hospitals with dataset D, a global loss Zhu and Jin (2019) function $f_j(w, x_i, y_i)$ minimizing the weights. The difference between the estimated and real for each hospital $f_j(w, x_i, y_i)$, the global model function of the $F(w)$ is described as

$$F(w) = \frac{1}{|M_I|} \sum_{i \in I} u_i \cdot F_i(w) = \frac{1}{|M_I|} \sum_{i \in I} \sum_{i \in D_i} u_i \cdot \frac{f_j(w, x_i, y_i)}{|D_i|} \quad (4)$$

Where i is sample dataset (x_i, y_i) of the gallery $I = \{1, 2, \cdots, n\}$ Tran et al. (2019) , u_i is the number of hospitals individual dataset models. In our proposed training process, we enhanced the accuracy of the model by iteratively minimizing the loss function of the global model. The equation of the loss function given as

$$Q(w, t) = \underset{i \in I, t \leq T}{\arg \min} F(w) \quad (5)$$

$$Pr(w_i \in \mathbb{R}_d) \leq \exp(\epsilon) Pr\left(w_i' \in \mathbb{R}_d\right) \quad (6)$$

$$\sum_{i=1}^{t} \Delta t(i) \leq \min(T_1, T_2, \ldots, T_n) \quad (7)$$

Where $Pr(w_i \in \mathbb{R}_d) \leq \exp(\epsilon) Pr\left(w_i' \in \mathbb{R}_d\right)$ is the privacy of the users Lu et al. (2019) of the parameters of the

$(T_1, T_2, \ldots, T_n)$. $\Delta t(i)$ is the execution time of the iteration.
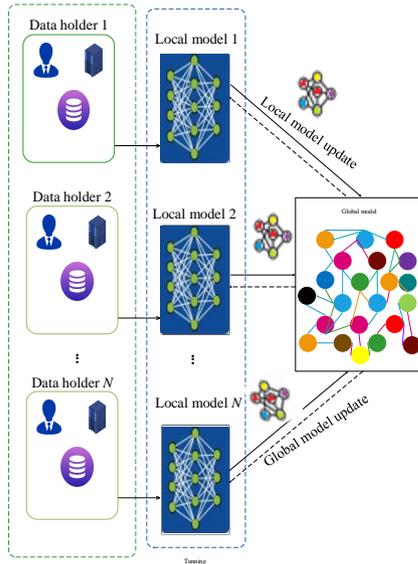

Fig. 2: Federated Learning Model

2.3. Homomorphic Encryption

Homomorphic encryption allows the calculation of encrypted data (ciphertext) without decryption. The new encrypted data matches the result of the operation performed on the unencrypted data after decryption. We utilized the BGV Brakerski et al. (2014) ncryption scheme, which takes as input the secret key with large noise and outputs an unencrypted data of the same data with a fixed amount of noise. Additionally, a key-switching procedure which text encrypt data and output the same message. We refer to the detailed encryption scheme for readers in Brakerski et al. (2014). Therefore, we used homomorphic encryption to encrypt the gradients Aono et al. (2017); Bottou (2010) to share the data in the blockchain distributed network. The previous research shares the encrypted gradients and shares to the centralized serverLi et al. (2015, 2014). They do not consider a distributed blockchain network. The problem of a blockchain database is cost-effective. For that reason, we use homomorphic to encrypt the model and train the local model to the global model.

We define Z is the unencrypted matrix data of the mini-batch dataset with the size of $S * T$, before the encryption of tensor, a private key matrix ϕ with size $S * S$ as:

$$
\begin{bmatrix}
\phi_{11} & \phi_{12} & \cdots & \phi_{1S} \\
\phi_{21} & \phi_{22} & \cdots & \phi_{2S} \\
\vdots & \vdots & \vdots & \vdots \\
\phi_{S1} & \phi_{S2} & \cdots & \phi_{SS}
\end{bmatrix}
\tag{8}
$$

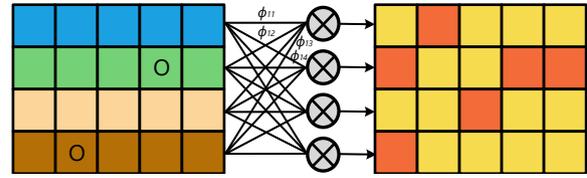This key only access by the users/participants who share the mini-batch dataset

Fig. 3: Homomorphic encryption

$$
\begin{bmatrix}
\mathbb{Z}_{(1)} \\
\mathbb{Z}_{(2)} \\
\vdots \\
\mathbb{Z}_{(S)}
\end{bmatrix}
=
\begin{bmatrix}
\phi_{11} & \phi_{12} & \cdots & \phi_{1S} \\
\phi_{21} & \phi_{22} & \cdots & \phi_{2S} \\
\vdots & \vdots & \vdots & \vdots \\
\phi_{S1} & \phi_{SS2} & \cdots & \phi_{SS}
\end{bmatrix}
\otimes
\begin{bmatrix}
Z_{(1)} \\
Z_{(2)} \\
\vdots \\
Z_{(N)}
\end{bmatrix}
\tag{9}
$$

where $Z(i)$ shows the vector data of the i_{th} node of the blockchain ledger. The $\otimes$ operator shows the product between two ciphertext

$$
\mathbb{Z}_{(i)} = \phi_{i1}Z_{(1)} + \phi_{i2}Z_{(2)} + \cdots + \phi_{iN}Z_{(S)}
\tag{10}
$$

The Figure 3 shows the homomorphic encryption function with the linear transformation of matrix. In this way, the linear transformation maintain the low rank functionality. The function $\phi_{ij} \in [0, 1)$, and $\sum_{j=1} \psi_{i,j} = 1$ shows the homomorphic encryption with private key.

2.4. Blockchain-Enabled Federated Learning

To train the better AI model for the industry 4.0 required to collect the data from multiple sources without leakage the privacy and authentication of the users. Therefore, we use federated learning with the blockchain distributed ledger to update the global AI model. The blockchain collects the data model from different nodes and aggregates the local and global model. The smart contract uploaded the weights and updated the models. The proposed architecture integrates blockchain with federated learning for full decentralization and enhancing security. Also, decentralization provides more accuracy of the model and enables the poisoning-attack-proof.

Some issues are not resolved for federated learning, i.e., insufficient incentives, poisoning attacks, etc. Therefore some authorsLu et al. (2020b); Qu et al. (2020) design the blockchain with the federated learning. Similarly, Pokhrel and Choi Pokhrel and Choi (2020) design a technique to protect privacy. The major issue of previous papers not including the encryption technique with the blockchain model gradients sharing. Therefore, this paper use the directed acyclic graph with the with the Proof-of-Work (PoW) consensus algorithm for the aggregation of gradients. Additionally, this work is fully decentralized and train accurate model without leakage the privacy of the user.

3. SECURE DATA SHARING FOR BLOCKCHAIN AND FEDERATED LEARNING

In this section, We first we introduce the high level architecture of the system and technical details in Figure 4. Our proposed scheme consist of multiple users share the data securely

using the federated learning with blockchain technology. The proposed architecture has multiple phases.

Local model:

1. Input COVID-19 images to train the model.
2. Learn the local model and calculate the local gradients.
3. Encrypt the gradients of the local model.

Send the weights to the blockchain network for aggregation model:

1. Aggregate $W_i(a) \leftarrow \frac{1}{\sum_{i \in S_t} |\mathcal{D}_i|} \sum_{i \in S_t} |\mathcal{D}_i| W_i(a)$ all users weights ciphertext.

Broadcast the weights:

1. Update the deep learning model based on global weights.
2. Upload the local model updates.

3.1. Training The Local Model For the COVID-19 dataset

In this section, we train the local model for detection of the COVID-19. The main model divided into three parts: (i) Segmentation Network (ii) Classification (iv) Probabilistic Grad-CAM Saliency Map Visualization

3.1.1. Segmentation network

Our segmentation network obtains the ground-truth lung masks and extracts the lung region using a learning method Liao et al. (2019); LaLonde and Bagci (2018). We removed the unnecessary or failure data manually, and the renaming segmentation data was taken as ground-truth masks. The 3D Lung mask is input the whole image for training and testing data. The training objective is to adopt the capsule network segmentation. Where $r_{t_i^\ell|xy}$ is the routing coefficient, $b_{t_i^\ell|xy}$ shows the pixel of images, s and y shows the ground truth label with the $\in$ {heart, background, left lung, right lung}.

$$r_{t_i^\ell|xy} = \frac{\exp\left(b_{t_i^\ell|xy}\right)}{\sum_k \exp\left(b_{t_i^\ell k}\right)} \quad (11)$$

To determine the final output of the segmentation using the non-linear squashing function

$$\mathbf{v}_{xy} = \frac{\left\|\boldsymbol{p}_{xy}\right\|^2}{1 + \left\|\boldsymbol{p}_{xy}\right\|^2} \frac{\boldsymbol{p}_{xy}}{\left\|\boldsymbol{p}_{xy}\right\|} \quad (12)$$

Where $\mathbf{v}_{xy}$ is the output of the segmented image with the spatial location (x, y) and $\boldsymbol{p}_{xy}$ is the final input.

3.1.2. Classification

We design a Capsule Network because it achieves high performance in detecting diseases in the medical images. The previous technique needs lots of data to train a more accurate model. The Capsule Network improves the deep learning models' performance inside the internal layers of the deep learning models. The architecture of our modified Capsule Network is similar to Hinton Capsule Network. The Capsule network contains four layers: i)convolutional layer, ii) hidden layer, iii) PrimaryCaps layer, and iv) DigitCaps layer.

A capsule is created when input features are in the lower layer. Each layer of the Capsule Network contains many capsules. To train the capsule network, the activation layer represents instantiate parameters of the entity and compute the length of the capsule network to re-compute the scores for the feature part. Capsule Networks is a better replacement for Artificial Neural Network (ANN). Here, the capsule acts as a neuron. Unlike ANN where a neuron outputs a scalar value, capsule networks tend to describe an image at a component level and associate a vector with each component. The probability of the existence of a component is represented by this vectors length and replaces max-pooling with "routing by agreement". As capsules are independents the probability of correct classification increases when multiple capsules agree on the same parameters. Every component can be represented by a pose vector U_i rotated and translated by a weighted matrix $W_{i,j}$ to a vector $\hat{u}_{i|j}$. Moreover, the prediction vector can be calculated as:

$$\hat{u}_{i|j} = W_{i,j} u_i \quad (13)$$

The next higher level capsule i.e., s_j processes the sum of predictions from all the lower level capsules with $c_{i,j}$ as a coupling coefficient. Capsules s_j can be represented as:

$$S_j = \sum_i c_{i,j} \hat{u}_{i|j} \quad (14)$$

where $c_{i,j}$ can be represented as a routing softmax function given as:

$$c_{i,j} = \frac{e^{b_{ij}}}{\sum_k e^{b_{ik}}} \quad (15)$$

As can be seen from the Figure 4, the parameter c, A squashing function is applied to scale the output probabilities between 0 and 1 which can be represented as:

$$a = \frac{\|a\|^2}{1 + \|a\|^2} \frac{a}{\|a\|} \quad (16)$$

For further details, refer to the original study Sabour et al. (2017).

3.1.3. CAM map visualization

We find the interpretability of the proposed capsule network by visualization of the COVID-19 slices. The most widely (GRAD-CAM) technique previous technique Selvaraju et al. (2017). More precisely,The GRAD-CAM map takes input as an image using the following equation.

$$l^c(x) = Upsampling\left(\sigma\left(\sum_M \alpha_M^c f^M(x)\right)\right) \in I \quad (17)$$

where I is the input image is the last layer of the convolution layer. Moreover, upsampling of the input image $m * n$ with the feature vector $u * v$. σ defined as the ReLU layer. However the probability of each pixel calculated by
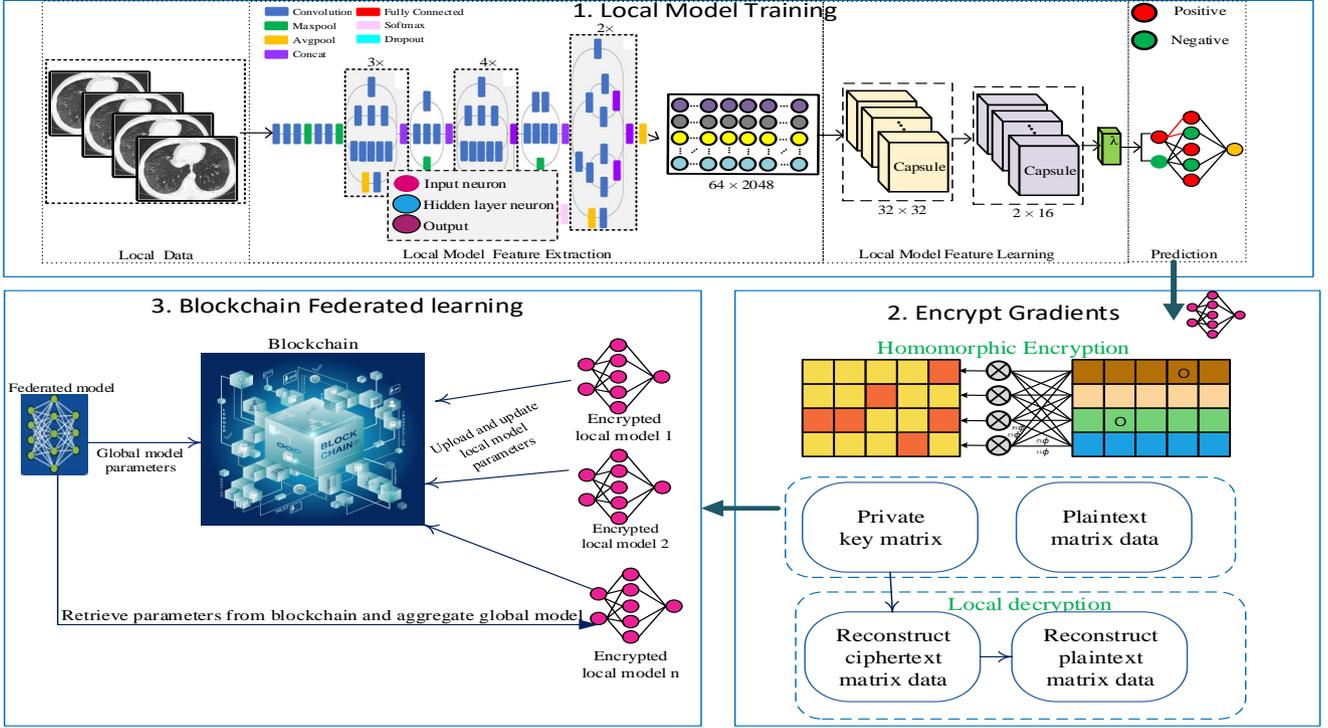
Fig. 4: Local Model: Deep Learning Model for COVID-19. We employ a modified version of inception V3 (IV3*)deep learning model as a feature extraction pipeline. Further, we train the extracted features using to layers of the capsule network. Encypt Gradiants: encrypt the weights. Blockcahin federated learning combine the local model.

$$\left[l^c_{prob}(x)\right]_i = \frac{1}{M_i}\left[\sum_{M=1}^{M} r^c(x_M)\,Q_M\left(l^c(x_M)\right)\right]_i \qquad (18)$$

Where K is the slice of the each image x pixel, $l^c(x_M)$ compute the GRAD-CAM by using the equation 17 with respect to frequency of the image. M is computed after the soft max layer of the capsule network. Equation 18 shows the average probability of the each pixel of the class for the global saliency map.

3.2. The Architecture of Gradients Encryption & Decryption

The data provider P, who holds the private medical images I, rain the local model and encrypt the local model vector. Then send to the blockchain network B. The blockchain federated learning model aggregates the encrypted vector using the global federated learning model. Moreover, the gradients encryption & decryption techniques for the secure weight sharing proposed by Lyubashevsky et al. ElGamal (1985) based on Ring-LWE scheme. Suppose $\Phi_n(X)$ is the reducible polynomial function The degree of the polynomial function $\phi(n)$, $R_p = R/pR$ and $R = \mathbb{Z}[X]/(\Phi_n(X))$ is the polynomial ring . The samples $(a, b = s \cdot a + e)$ of the Ring-LWE , where s, e indicates the Gaussian distribution.

Firstly, we define a ciphertext and plaintext space. Ring $R_p = (\mathbb{Z}/q\mathbb{Z})[X]/(\Phi_n(X))$ defined as plaintext with the modulus q. Similarity, $R_{p_1} = (\mathbb{Z}/p_1\mathbb{Z})\,|\,X]/(\Phi_n(X))$ defined as internal ciphertext RBGV and $R'_{p_1} = (\mathbb{Z}/p_1\mathbb{Z})[X]/(\Phi_{n'}(X))$ de-

fined as external ciphertext. However, the $\phi(n) = 2l\phi(n)$ with the $l = \lceil\log p_1\rceil$ and $p_1 = p \cdot p_0$ for primes p, p_0.

Then, we describe some widely used sampling subroutines for better readability as follows:

1. $\mathcal{ZV}(n)$: is represents as a vector space of the n numbers from $\{-1, 0, 1\}$ the probabilities of the each element are $Pr_{-1} = \frac{1}{4}, Pr_0 = \frac{1}{2}, Pr_1 = \frac{1}{4}$
2. $GM(n, \sigma)$: is represents as a vector space of the n numbers, the Gaussian distribution σ and standard deviation mean 0.
3. $\mathcal{VN}(n, p)$: is represents as a vector space of the n numbers from randomly uniform distribution modulo p.

3.2.1. Setup

Suppose $N \in N$ is number of devices, and K is the security parameter, For more details, the internal encryption defined as:

1. $Draw\,\tilde{a} \leftarrow \mathcal{VN}(\phi(n), p_1)$ and $\tilde{s}, \widetilde{\gamma} \leftarrow \mathcal{GM}(\phi(n), \tilde{\sigma})$.
2. Compute $b = \tilde{a} \cdot \tilde{s} + q \cdot \widetilde{\gamma}$
3. Output $pk = (a, b) \in R_{p_1} \times R_{p_1}$ as public key and $SK_{C_2} = \tilde{s} \in R_{p_1}$ as part of secret key for the distributed ledger blockchain.
4. Output $sk_i = s_i \in R'_{p_1}$ as secret key for participant i and $SK_{C_1} = -\sum_i s_i \in R'_{p_1}$ as another part of secret key for the distributed ledger blockchain.

3.2.2. Gradients encryption

In order to connection among the vector Z^n and ring R during encryption phase, the mappings as follows:

1. $Map_{R \to Z}n$: A coefficient representation of a input ring elements of n entities.
2. $Map_{\mathbb{Z}^n} \to R$: A matrix over the same ring as the vector containing the coefficients representations of the vector

Generation of internal ciphertext (e.g., RBGV)raining Local Models

3.2.3. The architecture of gradients encryption decryption for external ciphertext

1. Set $\mathbf{v}_i = Map\left(\widetilde{c}_{i,0}\|\widetilde{c}_{i,1}\right) \in \mathbb{Z}_{p_1}^{2\phi(n)}$
2. Invoke algorithm 1 to sample $\mathbf{e}_i \in \mathbb{Z}_{p1}^{2\phi(n)l}$ subject to the distribution $\Lambda_{\mathbf{v}_i}^{\perp}(\mathbf{G})$, where $\mathbf{e}_i = sample\left(v_{i_1}, \sigma\right)........sample\left(v_{i_2\phi(n)}, \sigma\right)$
3. Set $e_i = \left(Map_{\mathbb{Z}^{\phi(n')}) \to R'_{n!}}(\mathbf{e}_i)\right)$
4. Compute $c_i = a \cdot s_i + e_i \in R_{p1}$
5. Send final ciphertext c_i to the blockchain network.
6. Aggregate all the ciphertexts $c = \sum_i c_i = a \cdot \sum_i s_i + \sum_i e_i \in R'_{p_i}$ in the blockchain network
7. Compute the sum of errors terms $\$e = c + a \cdot SK_{C_1} = \sum_i e_i \in R'_{p_1}$,where $SK_{C_1} = -\sum_i s_i$.
8. Set $\mathbf{e} = Map_{R'_{p1} \to \mathbb{Z}^{\phi(n')}}(e)$

3.2.4. The architecture of gradients encryption decryption for internal ciphertext

1. Set $gd_i^t = Map_{\mathbf{Z}^{\phi(n)} \to R_q^{(}\mathbf{g}\mathbf{d}_i^t)} \in R_q$.
2. Draw $e_0, e_1 \leftarrow \mathcal{GS}(\phi(n), \sigma)$ and $v \leftarrow \mathcal{ZV}(\phi(n))$.
3. Compute $\widetilde{c}_{i,0} = \widetilde{b} \cdot \tilde{v} + q \cdot \widetilde{e}_0 + gd_i^t$ and $\widetilde{c}_{i,1} = \widetilde{a} \cdot \widetilde{v} + q\, e_1$ for modulus p_1.
4. Output internal ciphertext $\widetilde{c}_i = \left(\widetilde{c}_{i,0}, \widetilde{c}_{i,1}\right) \in R_{p_1} \times R_{p_1}$
5. Recover the sum of RBGV ciphertext by computing $\mathbf{v} = \sum_i \mathbf{v}_i = \mathbf{G} \cdot \mathbf{e} \bmod p_1 \in \mathbb{Z}_{p1}^{2\phi(n)}$
6. Split the vector $\mathbf{v} = (\mathbf{c}_0, \mathbf{c}_1) \in \mathbb{Z}_{p_1}^{\phi(n)} \times \mathbb{Z}_{p_1}^{\phi(n)}$.
7. Set $\tilde{c}_0 = Map_{\mathbb{Z}^{\phi(n)} \to R_{p_1}}(\mathbf{c}_0) \in R_{p_1}$ and $\tilde{c} = Map_{\mathbf{Z}^{\phi}(n) \to R_{p_1}}(\mathbf{c}_1) \in R_{p_1}$
8. Invoke algorithm Scale $((\widetilde{c}_o, \widetilde{c}_1), p_1, p_0)$ to switch modulus and produce the scaled ciphertext $\tilde{c}_o, \tilde{c}_1$ modulo p_0
9. Decrypt the ciphertext and produce the sum of plaintext by $gd^t = \sum_{i \in [N]} gd_i^t = \widetilde{c}_o - SK_{C_2} \cdot \tilde{c}_1 \mod q \in R_q$
10. Set$gd^t = Map_{R_q \to \mathbf{Z}^{\phi(n)}}\left(gd^t\right)$.
11. Broadcast the global gradients gd^t

3.3. Consensus in Permissioned Blockchain Federated Learning

The main goal of this section is to exaggeration of the global model with the blockchain DAG mechanism. The local DAG is responsible for synchronous global training via federated learning. However, the storage capability is improved to store the model in the DAG. Based on the federated learning and permissioned blockchain, the following steps to adjust the decentralized model aggravation. Firstly select the nodes of the users and then local train and encrypt the weights. Then aggregate the weights in the global model. The consensus (i.e., POW) for data sharing is high cost. To address the problem of the high

cost, we proposed a hybrid DAG based scheme is provided in Algorithm 2. However, we combine the update weight process of federated learning with the quality verification process using the blockchain DAG. The Algorithm 12 shows the global aggregation of the model gradients for the federated learning.

Algorithm 1: Global Federated Learning aggregation algorithm.

---

1 $\theta_{\text{global}}^{t-1} \leftarrow$ global model;

2 $\left\{G_{I(j)}^t\right\}_{j=1}^m \leftarrow$ legal gradient vectors;

3 $g_{global}^t \leftarrow 0$;

4 $l \leftarrow 0$;

5 **for** *k=1,2,..m* **do**

6   **if** $G_{I(k)}^t \neq \perp$ **then**

7   Compute $G_{\text{global}}^t \leftarrow G_{\text{global}}^t + \alpha_{I(k)} l_{l(k)} G_{I(k)}^t$;

8   Compute $\leftarrow l + \alpha_{I(k)} l_{l(k)}$

9   **end**

10   Compute $G_{global}^t \leftarrow \frac{1}{l} G_{global}^t$;

11   update $\theta_{\text{global}}^t \leftarrow \theta_{\text{global}}^{t-1} - \eta G_{\text{global}}$

12 **end**

3.3.1. The local directed acyclic graph (DAG)

The local DAG structure is used individually for the each user. In each iteration t represents federated learning, permissioned blockchain nodes are selected to verify the aggregation of model u_a. In local weight aggregation of deep learning model, weights $u_i \in u_P$ are transfer to the updated model $m_i(t)$ to the near by users. The model accuracy of weights $W(m_i(t))$ is calculated as

$$W\left(m_i(t)\right) = \frac{|d_i| + \rho \cdot \sum_j d_{m_j}}{\sum_{i=1}^N |d_i| + \sum_j d_{m_j}} \cdot s_i \cdot Acc\left(m_i(t)\right) \quad (19)$$

Where i is the local training and $|d_i|$ is the dataset size of the model, $\sum_j d_{m_j}$ represents the accumulated dataset size of the deep learning local model. S_i execute the each user training slots and $Acc\left(m_i(t)\right)$ shows the accuracy of the each trained model.

To verify the reliability of the transaction weights , we calculate weight transaction $CW(m_i(t))$

$$CW\left(m_i(t)\right) = W\left(m_i(t)\right) + \frac{1}{M} \sum_{j=1}^M \Delta Acc_j \cdot W(j) \quad (20)$$

Where $\Delta Acc_j = Acc_j\left(m_i(t)\right) - W\left(m_i(t)\right)$, $W(j)$ are the weight of the each transacation j, where $m_i(t)$. Acc_j verifies the accuracy of the $m_i(j)$

3.3.2. Add the transaction into the blockchain DAG

To add the transaction to the blockchain DAG to update the deep learning model, first required to validate the local model's two transaction accuracy. Then attach all hashes and generate a new block. The new block (new transaction) is updated the blockchain DAG, which can broadcast the nodes in the local

model blockchain DAG. The Markov-chain Monte Carlo prototype is used to check the probability of every step. The equation of the Markov-chain Monte Carlo is defined as :

$$E[f(x)] \approx \frac{1}{m} \sum_{i=1}^{m} f(x_i)$$

$$(x_0, x_1, \ldots, x_m) \sim MC(p)$$

$$(21)$$

3.3.3. Confirmation and consensus

The transactions are confirmed or validated based on the cumulative weights. This article utilized the weighted walk method based on credibility, which can validate the transaction by selecting the unverified transactions. When a new transaction is generated, two walkers will be added to the blockchain DAG to select the transaction. The more transaction has been pass for verification to achieve high cumulative weight for verification.

$$P_{xy} = \frac{e^{CW(y) - CW(x)}}{\sum_{z:z \to x} e^{CW(z) - CW(x)}} \qquad (22)$$

Where P_{xy} is the transition probability towards the unverified transaction of x and y. z defined as the neighboring node of transaction that belongs to x, and $y \in \{z : z \to x\}$

In this way, the complexity of the PoW is less than traditional PoW. The more and more transaction is executed then the DAG will be faster and safer.

Algorithm 2: Federated Learning Empowered with Blockchain Network

---

1   $D_1 \leftarrow \{M_1, m_2, \ldots, v_N\}$ dataset ;

2   $m_0 \leftarrow$ Initialize global weights with the permissioned blockchain BC and DAG ;

3   $r_0 \leftarrow$ select the users to $M_P \subset M_I$ by the node selection $\{r_1, r_2, \ldots, r_N\}$;

4   **for** $e \in [episode]$ **do**

5   Select the leader r_0 ;

6   **for** $t \in [timeslot]$ **do**

7   **for** D_i dataset $\in M_p$ **do**

8   m_i matrix global model M_{t-1} from permissioned blockchain BC ;

9   m_i = local traning $w_i(t) = w(t) - \eta \cdot \nabla F_i(w_{t-1})$;

10   m_i = get local models updates DAG;

11   m_i run the local aggregation model and get the updated local model mi_t ;

12   m_i add the transactions to the DAG ;

13   **end**

14   **end**

15      $r0 \leftarrow (t) = \frac{\sum_{i=1}^{N} C_i w_i(t)}{\sum_{i=1}^{N} C_i}$ DAG blockchain updated the model , and averaging the models into $M(e)$;

16      $r0$ broadcasts model $M(e)$ to other nodes for verification, add all the transacations into the blockchain ledger ; $r0$ include the $M(e)$ global model form the blockchain ledger;

17 **end**

---

4. SECURITY ANALYSIS AND PERFORMANCE ANALYSIS

4.1. Dataset

In the past, Artificial intelligence (AI) has gained a reputable position in the field of clinical medicine. And in such chaotic situations, AI can help the medical practitioners to validate the disease detection process, hence increasing the reliability of the diagnosis methods and save precious human lives. Currently, the biggest challenge faced by AI-based methods is the availability of relevant data. AI cannot progress without the availability of abundant and relevant data.

In this paper, we introduce a small new dataset related to the latest family of coronavirus i.e. COVID-19. Such datasets play an important role in the domain of artificial intelligence for clinical medicine related applications. This data set contains the Computed Tomography scan (CT) slices for 89 subjects. Out of these 89 subjects, 68 were confirmed patients (positive cases) of the COVID-19 virus, and the rest 21 were found to be negative cases. The proposed dataset CC-19 contains 34,006 CT scan slices (images) belonging to 89 subjects out of which 28,395 CT scan slices belong to positive COVID-19 patients. This dataset is made publicly available via GitHub (https://github.com/abdkhanstd/COVID-19). Figure 5 shows some 2D slices taken from CT scans of the CC-19 dataset. Moreover, some selected 3D samples from the dataset are shown in Figure 6. The Hounsfield unit (HU) is the measurement of CT scans radiodensity as shown in Table 3. Usually, CT scanning devices are carefully calibrated to measure the HU units. This unit can be employed to extract the relevant information in CT Scan slices. The CT scan slices have cylindrical scanning bounds. For unknown reasons, the pixel information that lies outside this cylindrical bound was automatically discarded by the CT scanner system. But fortunately, this discarding of outer pixels eliminates some steps for preprocessing.
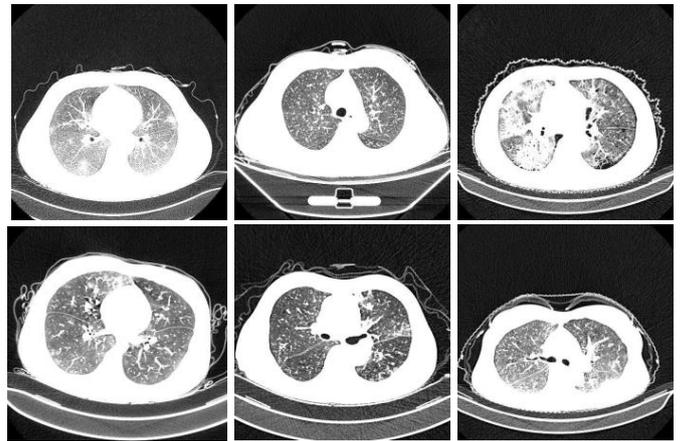

Fig. 5: Some random samples of CT scan 2D slices taken from CC-19 dataset.

Collecting dataset is a challenging task as there are many ethical and privacy concerns observed the hospitals and medical practitioners. Keeping in view these norms, this dataset was collected in the earlier days of the epidemic from various

Table 2: CC-19 dataset collected from three different hospitals (A, B, and C).

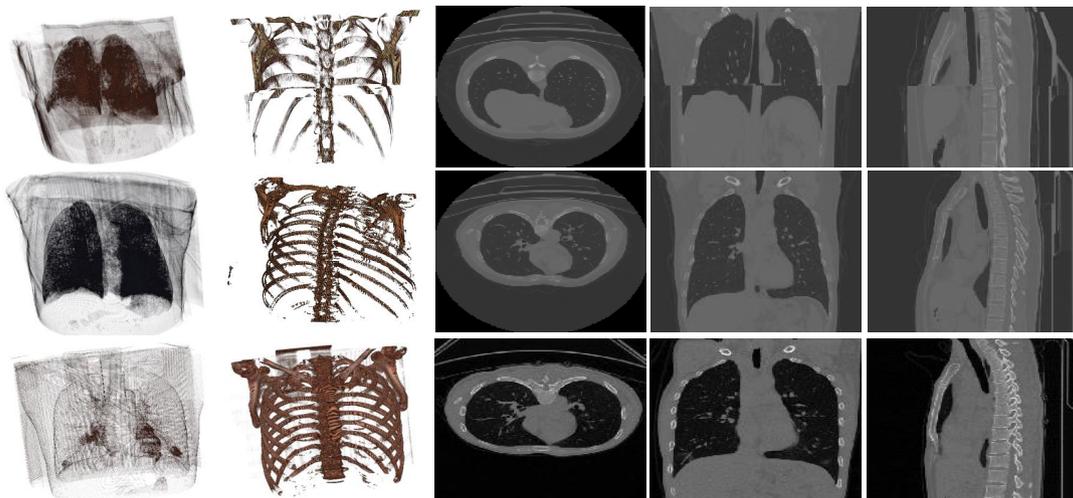| Hospital ID	A	A	B	B	C	C
CT scanner ID	1	2	3	4	5	6
Number of Patients	30	10	13	7	20	9
Infecation annotation	Voxel-level	Voxel-level	Voxel-level	Voxel-level	Voxel-level	Voxel-level
CT scanner	SAMATOM scope	Samatom Definitation Edge	Brilliance 16P iCT	Brilliance iCT	Brilliance iCT	GE 16-slice CT scanner
Lung Window level (LW)	-600	-600	-600	-600	-600	-500
Lung Window Witdh (WW)	1200	1200	1600	1600	1600	1500
Slice thickness (mm)	5	5	5	5	5	5
Slice increment (mm)	5	5	5	5	5	5
Collimation(mm)	128*0.6	16*1.2	128*0.625	16*1.5	128*0.6	16*1.25
Rotation time (second)	1.2	1.0	0.938	1.5	1.0	1.75
Pitch	1.0	1.0	1.2	0.938	1.75	1.0
Matrix	512*512	512*512	512*512	512*512	512*512	512*512
Tube Voltage (K vp)	120	120	120	110	120	120

Fig. 6: This figure shows some selected samples from the "CC-19 dataset". Each row represents different patient samples with various Hounsfield Unit (HU) for CT scans. The first column, from left to right, shows the lungs in the 3D volume metric CT scan sphere. The second column shows the extracted bone structure using various HU values followed by the XY, XZ, and YZ plane view of the subjects' CT scan. It is worth noting that the 3D volumetric representation is not pre-processed to remove noise and redundant information.

S/No	Substance	Hounsfield Unit (HU)
1	Air	-1000
2	Bone	+700 to +3000
3	Lungs	-500
4	Water	0
5	Kidney	30
6	Blood	+30 to +45
7	Grey matter	+37 to +45
8	Liver	+40 to +60
9	White matter	+20 to +30
10	Muscle	+10 to +40
11	Soft Tissue	+100 to +300
12	Fat	-100 to -50
13	Cerebrospinal fluid(CSF)	15

Table 3: Various values of Hounsfield unit (HU) for different substances.

hospitals in Chengdu, the capital city of Sichuan. Initially, the dataset was in an extremely raw form. We preprocessed the data and found many discrepancies with most of the collected CT scans. Finally, the CT scans, with discrepancies, were discarded from the proposed dataset. All the CT scans are different from each other i.e. CT scans have a different number of slices for different patients. We believe that the possible reasons behind the altering number of slices are the difference in height and body structure of the patients. Moreover, upon inspecting various literature, we found that the volume of the lungs of an adult female is, comparatively, ten to twelve percent smaller than a male of the same height and age Bellemare et al. (2003).

4.2. Security Analysis's

The use of permissioned blockchain distributed technology achieved a secure mechanism for the various devices. We integrate the consensus blockchain process with the federated learning to address the trust of the security threats and privacy of the data.

1. **To Achieve the Differential Privacy:** According to the privacy of users, our proposed protocol is used to indistinguishable for the random values. We select the random vector for generation of the ciphertext $\widetilde{c_i}$, using the BGV scheme [31]. Where K is indistinguishable security parameter for the random values. Then v_i is transfer from the polynomial $\widetilde{c_i}$, for random values.

2. **Data Access:** The proposed technique is used federated learning with blockchain technology, the core idea is to develop the privacy of the data. The proposed model achieves data privacy by aggregating the encrypted technique with blockchain, which grantee the privacy protection of the data

3. **Aggregator the model trust security:** To aggregated sum of weights, the blockchain and local model client provide the security as fallows :

   3..1 Setup: First setup the security algorithm to generate the public parameters for the model

   3..2 Encrypt: client specify the parameter (i, m), Where i is the index of the entity and m is the plaintext. Finally, it returns the $Enc(i, m)$ value to the model.

   3..3 Compromise: The model comprises an i entity, then aggregated model returns the secret keys SK_c , this phase repeat many times.

   3..4 Challenge: It is allow only once throughout in the entire cycle. for every $i \in K$ generate and send two plain text m_1 and m_2. If bit is equal to 0 then compute the $c_i = Enc(m_i)$. Otherwise it will encrypted in the same way and send c_i
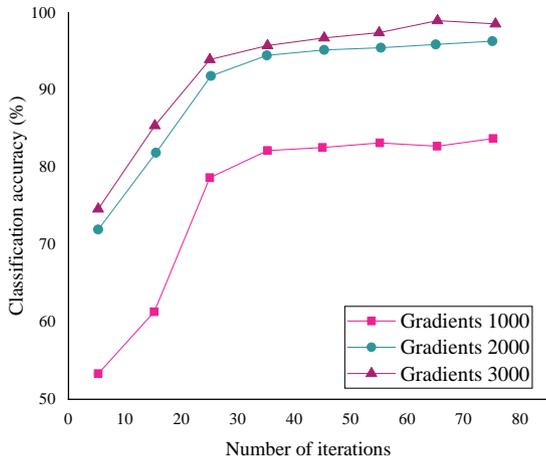
   3..5 Guess: The final output is 1 or 0

4. **Removing Centralized Trust:** The blockchain mechanism remove the third party trust and allows to users or hospitals commented with the decentralized network.

5. **Secure Data Management:** Only data trusted data provider upload the data to the network to ensure the reliability of the model. Moreover, the cryptography algorithm guarantee the security of the data.

6. **Guarantee the Quality of Shared Model:** To prevent the quality of the model, consensus process guarantee the quality of learned data.
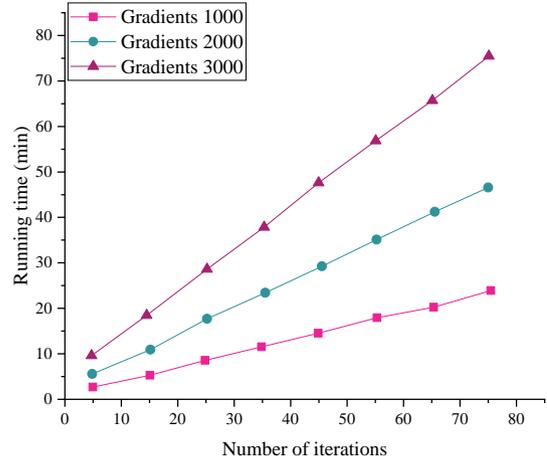
4.3. Performance Analysis

To evaluate the proposed method's performance, we adopted the federated learning model as a classifier to conduct the experimentation. We analyze and evaluate our model in terms of accuracy. The deep learning model; contains fully connected convolutional layers, where each of the layers consists of 128 neurons. Two factors affect the accuracy and running time of the federated learning model: the number of hospitals and gradients per hospital. We analyzed both factors on different ranges of values, as shown in Fig. 7 and Fig. 8, respectively. shows the execution time and accuracy with a different number of iteration. Here the number of iteration indicates the completed update of parameters. We compared the effect with the different number of gradients per hospital, and we distributed data to over six hospitals. To conduct the experimentation on basic setting, we only assumed the condition where no user has dropped out. It can be clearly seen that increasing the number of gradients per hospital leads towards higher accuracy, whereas it causes the computation overhead as shown in Fig. 7b. Therefore, to reduce the computation overhead in a practical environment, an appropriate number of gradients can be empirically chosen. In terms of model iterations, it can be observed that model accuracy converges after a certain number of iterations.

The required time to train the local model (local gradients) also depends on the size of the data and the number of selected hospitals. We analyzed the accuracy over a different number of users to train the model. The classification accuracy and execution time can be seen in Fig. 8. Similar to the previous observation, naturally increasing numbers of iterations and hospitals consume high computation cost. However, due to independent gradient computation on each user, the number of hospitals leads to high accuracy. Basically, the data is split into many chunks as per hospital; therefore, the local gradient will be calculated and combined to produce high accuracy.

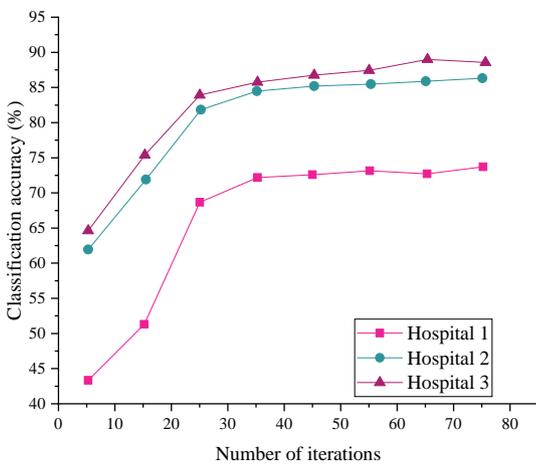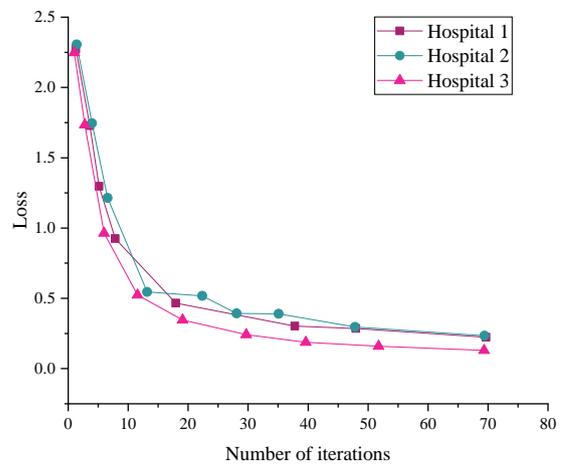(a)   (b)

Fig. 7: Hospitals=3 , no dropout, classification accuracy and running time for the various number of gradients per hospital.

(a)   (b)

Fig. 8: Gradient=1000, no dropout, classification accuracy and loss for various numbers of hospitals.

4.4. Local Model Capsule Network Performance Analysis

In this section we analysis the local deep learning models which is divided into three parts (i) Segmentation (ii) Classification (iii) Attention Map visualization

4.4.1. Segmentation network results

Capsule network lesion localization of the lung's COVID-19 region is shown in Figure 9. We extract the region of the lung of COVID-19 patients. We fix the parameters of the blockchain based federated learning, where total communication cost T to 300 and validate the each model in every round to select the best local model from the blockchain nodes. Moreover, we set the Adam optimizer learning rate of 0.0001. Each round contain 300 iteration with a batch size 4. Table 4 shows the federated learning model for the three hospitals. First three rows shows the (I/II/II) shows the hospitals. We compute the avrage of three hospital accuracy in "global test avg". This measure shows the global model , and blockchain nodes as major metric for performance evaluation.
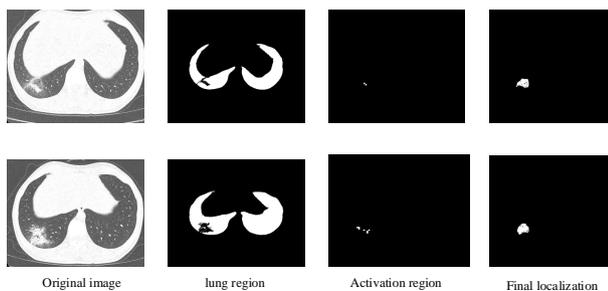

Fig. 9: Activation mapping algorithm segmentation results

Original image   lung region   Activation region   Final localization

4.4.2. Comparison the global and local model

This article conducts results from global and local deep learning models, i.e.,(Local I, Local II, Local III, Fed AVG. Fed Global, FedProx). We used deep learning models and different layers for comparing the performance models on the COVID-19 dataset, which is shown in Figure 10. We evaluate the performance of the capsule network for the detection of COVID-19 lung CT image accuracy. Figure 10 shows the local and global models; the global model achieves high high detection performance through the network. These models were tested using three different test lists containing about 11,450 CT scan slices.

4.4.3. Visualizations of the attention map regions

To understand the deeper, we calculate the probabilistic CAM to each CT image of COVID-19. The capsule network visualizes the patient CT images from the normal and COVID-19 classes, and a noticeable activation map is shown in Figure 11. Moreover, the applied CAM LaLonde and Bagci (2018); Liao et al. (2019) function visualize each image slice. These results strongly support our claim that the probabilistic Grad-CAM saliency map. These results strongly support our claim that the probabilistic Grad-CAM saliency map.
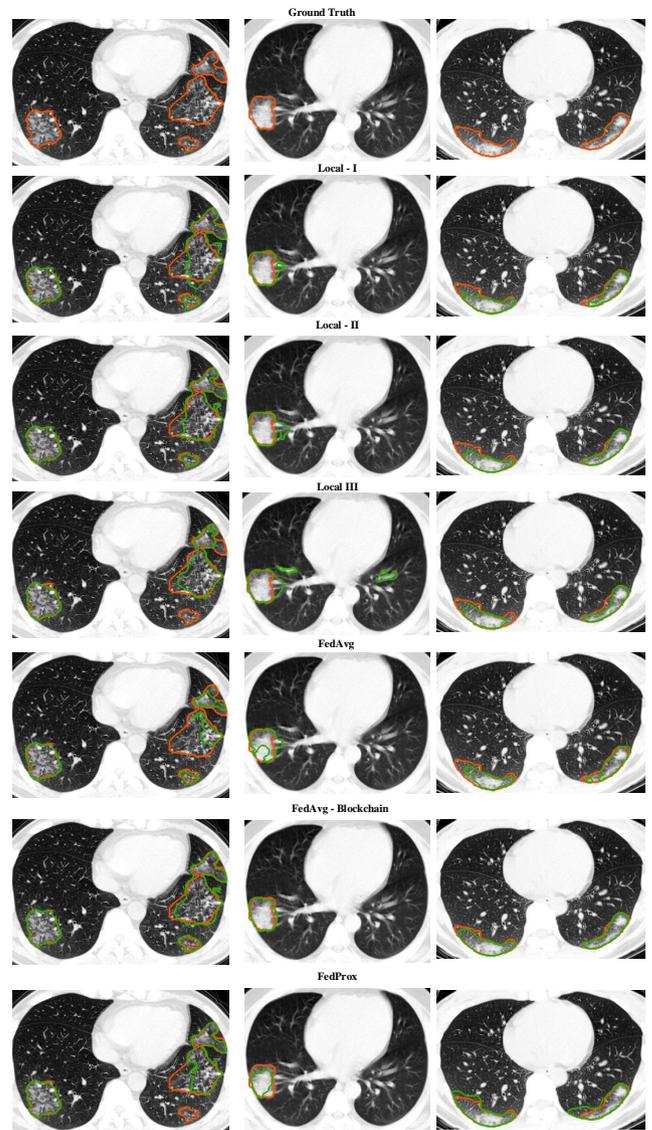

Fig. 10: Activation mapping algorithm segmentation results

4.5. Compare with other methods

To prove the local model accuracy and effectiveness of the proposed model. As we can observe capsule network achieved 98% accuracy in the detection of the COVID-19 CT scans. Although Han el al. also achieve 98% accuracy, they do not consider the data sharing techniques. Furthermore, we compare our scheme with the security analysis shown in Table 5. However, Bonawitz et al. Bonawitz et al. (2017)design a privacy-preserving framework to secure the gradients' aggregation using the federated learning global model. Zhang et al. Zhang et al. (2017) present the homomorphic encryption (HE) scheme and threshold secret sharing to secure the gradients. However, the shared model has no certainty about authentic users. In other words, the trust issue between different sources still exists; the proposed approach fill this gap and achieve trust between parties.

Table 4: COVID-19 lesion segmentation. Global test avg shows the Federated Learning global model. *n* spices the number of patients.

Parameters	Local - I	Local - II	Local III	FedAvg	FedAvg - Blockchain	FedProx
I (*n*=40)	80.2	64.12	57.0	82.13	78.93	82.53
II (*n*=20)	84.02	82.15	74.74	85.99	86.51	87.18
III (*n*=17)	74.00	72.38	88.05	82.72	87.18	82.65
global test avg	85.99	82.15	73.16	83.61 ±0.18	84.21 ± 0.43	84.12 ± 0:58
local avg	84.07			84.67	84.44	61.99
local gen	70.99			81.0	81.48	80.53

Fig. 11: Visualizations of the attention map regions

Study	Block-chain	Ser-ver	Data au-thenti-cation	Privacy / En-cryp-tion Data	Data Ac-cess	Centra-lized Trust
OURs	Yes	No	Yes	Yes	Yes	Yes
Kim et al. (2019)	Yes	No	Yes	No	Yes	Yes
Lu et al. (2020c)	Yes	No	Yes	No	Yes	Yes
Lu et al. (2020a)	Yes	No	Yes	No	Yes	Yes
Xu et al. (2019)	No	Yes	No	Yes	Yes	No
Yang et al. (2014)	No	Yes	No	Yes	Yes	No

Table 5: Compression with the security analysis

5. Conclusion

This article proposed a secure data sharing scheme for the distributed multiple hospitals for the internet of things applications, which incorporate local model training and secure global training. We secure the local model through the homomorphic encryption scheme, which helps build an intelligent model without leakage the data provider's privacy and create trust in the data training process. However, the blockchain-based algorithm aggregates the local model updates and provides the authentication of the data. The experiment results confirm the accuracy and effectiveness of the model. In future work, to enhance the latency of the blockchain and minimize the cost-effective solution.

References

Aono, Y., Hayashi, T., Wang, L., Moriai, S., et al., 2017. Privacy-preserving deep learning via additively homomorphic encryption. IEEE Transactions on Information Forensics and Security 13, 1333–1345.

Baheti, P., Sikka, M., Arya, K.V., Rajesh, R., 2020. Federated learning on distributed medical records for detection of lung nodules, in: Farinella, G.M., Radeva, P., Braz, J. (Eds.), Proceedings of the 15th International Joint Conference on Computer Vision, Imaging and Computer Graphics Theory and Applications, VISIGRAPP 2020, Volume 4: VISAPP, Valletta, Malta, February 27-29, 2020, SCITEPRESS. pp. 445–451.

Bellemare, F., Jeanneret, A., Couture, J., 2003. Sex differences in thoracic dimensions and configuration. American journal of respiratory and critical care medicine 168, 305–12.

Blanquer, I., Brasileiro, F.V., Brito, A., Calatrava, A., Carvalho, A., Fetzer, C., Figueiredo, F., Guimarães, R.P., Marinho, L.B., Jr., W.M., da Silva, A.S., Alberich-Bayarri, A., Camacho-Ramos, E., Jimenez-Pastor, A., Ribeiro, A.L.L., Nascimento, B.R., Silva, F., 2020. Federated and secure cloud services for building medical image classifiers on an intercontinental infrastructure. Future Gener. Comput. Syst. 110, 119–134.

Bonawitz, K., Ivanov, V., Kreuter, B., Marcedone, A., McMahan, H.B., Patel, S., Ramage, D., Segal, A., Seth, K., 2017. Practical secure aggregation for privacy-preserving machine learning, in: Proceedings of the 2017 ACM SIGSAC Conference on Computer and Communications Security, pp. 1175–1191.

Bottou, L., 2010. Large-scale machine learning with stochastic gradient descent, in: Proceedings of COMPSTAT'2010. Springer, pp. 177–186.

Brakerski, Z., Gentry, C., Vaikuntanathan, V., 2014. (leveled) fully homomorphic encryption without bootstrapping. ACM Transactions on Computation Theory (TOCT) 6, 1–36.

Brisimi, T.S., Chen, R., Mela, T., Olshevsky, A., Paschalidis, I.C., Shi, W., 2018. Federated learning of predictive models from federated electronic health records. Int. J. Medical Informatics 112, 59–67.

Can, Y.S., Ersoy, C., 2021. Privacy-preserving federated deep learning for wearable iot-based biomedical monitoring. ACM Trans. Internet Techn. 21, 21:1–21:17.

Cheng, Y., Liu, Y., Chen, T., Yang, Q., 2020. Federated learning for privacy-preserving AI. Commun. ACM 63, 33–36.

Dai, H.N., Zheng, Z., Zhang, Y., 2019. Blockchain for internet of things: A survey. IEEE Internet of Things Journal 6, 8076–8094.

Das, N.N., Kumar, N., Kaur, M., Kumar, V., Singh, D., 2020. Automated deep transfer learning-based approach for detection of covid-19 infection in chest x-rays. Irbm .

Deng, J., Cai, J., Aftab, M.U., Khokhar, M.S., Kumar, R., et al., 2020. Visual features with spatio-temporal-based fusion model for cross-dataset vehicle re-identification. Electronics 9, 1083.

Deng, J., Khokhar, M.S., Aftab, M.U., Cai, J., Kumar, R., Kumar, J., et al., 2021. Trends in vehicle re-identification past, present, and future: A comprehensive review. arXiv preprint arXiv:2102.09744 .

Dinh, C.T., Tran, N.H., Nguyen, M.N.H., Hong, C.S., Bao, W., Zomaya, A.Y., Gramoli, V., 2021. Federated learning over wireless networks: Convergence analysis and resource allocation. IEEE/ACM Trans. Netw. 29, 398–409.

ElGamal, T., 1985. A public key cryptosystem and a signature scheme based on discrete logarithms. IEEE transactions on information theory 31, 469–472.

Huang, L., Shea, A.L., Qian, H., Masurkar, A., Deng, H., Liu, D., 2019. Patient clustering improves efficiency of federated machine learning to predict mortality and hospital stay time using distributed electronic medical records. J. Biomed. Informatics 99.

Khan, A.A., Shafiq, S., Kumar, R., Kumar, J., Haq, A.U., 2020. H3dnn: 3d deep learning based detection of covid-19 virus using lungs computed tomography, in: 2020 17th International Computer Conference on Wavelet Active Media Technology and Information Processing (ICCWAMTIP), IEEE. pp. 183–186.

Kim, H., Park, J., Bennis, M., Kim, S.L., 2019. Blockchained on-device federated learning. IEEE Communications Letters 24, 1279–1283.

Kumar, R., Khan, A.A., Kumar, J., Zakria, A., Golilarz, N.A., Zhang, S., Ting, Y., Zheng, C., Wang, W., 2021a. Blockchain-federated-learning and deep learning models for covid-19 detection using ct imaging. IEEE Sensors Journal .

Kumar, R., Wang, W., Kumar, J., Yang, T., Khan, A., Ali, W., Ali, I., 2021b. An integration of blockchain and ai for secure data sharing and detection of ct images for the hospitals. Computerized Medical Imaging and Graphics 87, 101812.

LaLonde, R., Bagci, U., 2018. Capsules for object segmentation. arXiv preprint arXiv:1804.04241 .

Lee, G., Shin, S., 2020. Reliability and performance assessment of federated learning on clinical benchmark data. CoRR abs/2005.11756.

Li, H., Liu, D., Dai, Y., Luan, T.H., Shen, X.S., 2014. Enabling efficient multi-keyword ranked search over encrypted mobile cloud data through blind storage. IEEE Transactions on Emerging Topics in Computing 3, 127–138.

Li, H., Liu, D., Dai, Y., Luan, T.H., Yu, S., 2015. Personalized search over encrypted data with efficient and secure updates in mobile clouds. IEEE Transactions on Emerging Topics in Computing 6, 97–109.

Li, X., Gu, Y., Dvornek, N.C., Staib, L.H., Ventola, P., Duncan, J.S., 2020. Multi-site fmri analysis using privacy-preserving federated learning and domain adaptation: ABIDE results. Medical Image Anal. 65, 101765.

Liao, F., Liang, M., Li, Z., Hu, X., Song, S., 2019. Evaluate the malignancy of pulmonary nodules using the 3-d deep leaky noisy-or network. IEEE transactions on neural networks and learning systems 30, 3484–3495.

Lu, Y., Huang, X., Dai, Y., Maharjan, S., Zhang, Y., 2019. Differentially private asynchronous federated learning for mobile edge computing in urban informatics. IEEE Transactions on Industrial Informatics 16, 2134–2143.

Lu, Y., Huang, X., Dai, Y., Maharjan, S., Zhang, Y., 2020a. Blockchain and Federated Learning for Privacy-Preserved Data Sharing in Industrial IoT. IEEE Transactions on Industrial Informatics 16, 4177–4186. doi:10.1109/TII.2019.2942190.

Lu, Y., Huang, X., Zhang, K., Maharjan, S., Zhang, Y., 2020b. Blockchain empowered asynchronous federated learning for secure data sharing in internet of vehicles. IEEE Transactions on Vehicular Technology 69, 4298–4311.

Lu, Y., Huang, X., Zhang, K., Maharjan, S., Zhang, Y., 2020c. Blockchain Empowered Asynchronous Federated Learning for Secure Data Sharing in Internet of Vehicles. IEEE Transactions on Vehicular Technology 69, 4298–4311. doi:10.1109/TVT.2020.2973651.

Malekzadeh, M., Hasircioglu, B., Mital, N., Katarya, K., Ozfatura, M.E., Gündüz, D., 2021a. Dopamine: Differentially private federated learning on medical data. CoRR abs/2101.11693.

Malekzadeh, M., Hasircioglu, B., Mital, N., Katarya, K., Ozfatura, M.E., Gündüz, D., 2021b. Dopamine: Differentially private federated learning on medical data. CoRR abs/2101.11693.

Pathak, Y., Shukla, P.K., Tiwari, A., Stalin, S., Singh, S., 2020. Deep transfer learning based classification model for covid-19 disease. Irbm .

Pokhrel, S.R., Choi, J., 2020. Federated learning with blockchain for autonomous vehicles: Analysis and design challenges. IEEE Transactions on Communications .

Qu, Y., Gao, L., Luan, T.H., Xiang, Y., Yu, S., Li, B., Zheng, G., 2020. Decentralized privacy using blockchain-enabled federated learning in fog computing. IEEE Internet of Things Journal .

Sabour, S., Frosst, N., Hinton, G.E., 2017. Dynamic routing between capsules, in: Advances in Neural Information Processing Systems 30: Annual Conference on Neural Information Processing Systems 2017, 4-9 December 2017, Long Beach, CA, USA, pp. 3856–3866.

Selvaraju, R.R., Cogswell, M., Das, A., Vedantam, R., Parikh, D., Batra, D., 2017. Grad-cam: Visual explanations from deep networks via gradient-based localization, in: Proceedings of the IEEE international conference on computer vision, pp. 618–626.

Shokri, R., Shmatikov, V., 2015. Privacy-preserving deep learning, in: Proceedings of the 22nd ACM SIGSAC conference on computer and communications security, pp. 1310–1321.

Tang, W., Ren, J., Zhang, Y., 2018. Enabling trusted and privacy-preserving healthcare services in social media health networks. IEEE Transactions on Multimedia 21, 579–590.

Thomas, M.A., Abraham, D.S., Liu, D., 2018. Federated machine learning for translational research, in: 24th Americas Conference on Information Systems, AMCIS 2018, New Orleans, LA, USA, August 16-18, 2018, Association for Information Systems. URL: https://aisel.aisnet.org/amcis2018/Health/Presentations/34.

Thwal, C.M., Thar, K., Tun, Y.L., Hong, C.S., 2021. Attention on personalized clinical decision support system: Federated learning approach, in: Unger, H., Kim, J., Kang, U., So-In, C., Du, J., Saad, W., Ha, Y., Wagner, C., Bourgeois, J., Sathitwiriyawong, C., Kwon, H., Leung, C.K. (Eds.), IEEE International Conference on Big Data and Smart Computing, BigComp 2021, Jeju Island, South Korea, January 17-20, 2021, IEEE. pp. 141–147.

Tran, N.H., Bao, W., Zomaya, A., NH, N.M., Hong, C.S., 2019. Federated learning over wireless networks: Optimization model design and analysis, in: IEEE INFOCOM 2019-IEEE Conference on Computer Communications, IEEE. pp. 1387–1395.

Xu, G., Li, H., Liu, S., Yang, K., Lin, X., 2019. Verifynet: Secure and verifiable federated learning. IEEE Transactions on Information Forensics and Security 15, 911–926.

Yang, D., Xu, Z., Li, W., Myronenko, A., Roth, H.R., Harmon, S.A., Xu, S., Turkbey, B., Turkbey, E., Wang, X., Zhu, W., Carrafiello, G., Patella, F., Cariati, M., Obinata, H., Mori, H., Tamura, K., An, P., Wood, B.J., Xu, D., 2021. Federated semi-supervised learning for COVID region segmentation in chest CT using multi-national data from china, italy, japan. Medical Image Anal. 70, 101992.

Yang, K., Jia, X., Ren, K., 2014. Secure and verifiable policy update outsourcing for big data access control in the cloud. IEEE Transactions on Parallel and Distributed Systems 26, 3461–3470.

Yang, Q., Liu, Y., Chen, T., Tong, Y., 2019. Federated machine learning: Concept and applications. ACM Trans. Intell. Syst. Technol. 10, 12:1–12:19.

Yang, W., Liu, B., Lu, C., Yu, N., 2020. Privacy preserving on updated parameters in federated learning, in: ACM TUR-C'20: ACM Turing Celebration Conference, Hefei, China, May 22-24, 2020, ACM. pp. 27–31.

Zhang, X., Ji, S., Wang, H., Wang, T., 2017. Private, yet practical, multiparty deep learning, in: 2017 IEEE 37th International Conference on Distributed Computing Systems (ICDCS), IEEE. pp. 1442–1452.

Zhu, H., Jin, Y., 2019. Multi-objective evolutionary federated learning. IEEE transactions on neural networks and learning systems 31, 1310–1322.

Rajesh Kumar was born in Sindh Province of Pakistan in November 1991. He received his B.S. and M.S. degree in computer science from University of Sindh, Jamshoro, Pakistan. He received his Ph.D. in computer science and engineering from the University of Electronic Science and Technology of China (UESTC). He has currently Full time reseacher in Yangtze Delta Region Institute (Huzhou), University of Electronic Science and Technology of China. His research interests include machine learning, deep leaning, malware detection, Internet of Things (IoT) and blockchain technology. In addition, he has published more than 30 articles in various International journals and conference proceedings.

Professor Wenyong Wang eceived the B.S. degree in computer science from Beihang University, Beijing, China, in 1988, and the M.S. and Ph.D. degrees from the University of Electronic Science and Technology (UESTC), Chengdu, China, in 1991 and 2011, respectively. He has been a Professor with the School of Computer Science and Engineering, UESTC, in 2009. He has served as the Director of the Information Center of UESTC and the Chairman of the UESTC-Dongguan Information Engineering Research Institute, from 2003 to 2009. He is currently a Visiting Professor with the Macau University of Technology. His main research interests include next-generation Internet, software-designed networks, software engineering, and artificial intelligence. He is a member of the expert board of CERNET and China Next-Generation Internet Committee and a Senior Member of the Chinese Computer Federation.

Jay Kumar is currently a Ph.D student and working in Data Mining Lab, School of Computer Science and Engineering, University of Electronics Science and Technology of China. He received his Masters degree from Quaid-i-Azam University, Islamabad in 2018. His main interest of research include Text Mining, Data Stream Mining and Natural language processing. His current research work has been published in top conference of ACL, Journal of Information Sciences and IEEE transactions in Cybernetics.

Zakria received the M.S. degree in Computer Science and Information from N.E.D University in 2017. His Ph.D. degree with the School of Information and Software Engineering, University of Electronic Science and Technology of China. He has currently pursing Post Doctor in University of Electronic Science and Technology of China. He has a vast academic, technical, and professional experience in Pakistan. His research interests include artificial intelligence, computer vision particularly vehicle re-identification.

Abdullah Aman Khan received his master's degree in the field of Computer Engineering form National University of Science and Technology (NUST), Punjab, Pakistan in 2014. He is currently perusing PhD degree in the field of Computer Science and Technology form the school of computer science and engineering, University of Electronic Science and Technology, Sichuan, Chengdu, P.R. China. His main area of research includes electronics design, machine vision and intelligent systems.

Zheng Chengyu is working as senior engineer and general manager of China Telecom Company Limited. He graduated from Huazhong University of Science and Technology, majoring in computer software design. He pursued executive master's in business administration from Southwest University of Finance and Economics. He was selected by China Telecom Corporation to study at Stanford University in the United States. His main research directions include information technology system architecture design, mobile communication networks and buildin